

Modulation of High-Order Harmonic Generation from a Monolayer ZnO by Co-rotating Two-Color Circularly Polarized Laser Fields

Yue Qiao(乔月)^{1,2,3}, Jiaqi Chen(陈家祺)¹, Shushan Zhou(周书山)⁴,
Jigen Chen(陈基根)^{1*}, Shicheng Jiang(蒋士成)^{5*}, and Yujun Yang(杨玉军)^{2,3*}

¹School of Materials Science and Engineering, Taizhou University, Jiaojiang 318000, China

²Institute of Atomic and Molecular Physics, Jilin University, Changchun 130012, China

³Jilin Provincial Key Laboratory of Applied Atomic and Molecular Spectroscopy (Jilin University),
Changchun 130012, China

⁴School of Physics and Electronic Technology, Liaoning Normal University, Dalian 116029, China

⁵State Key Laboratory of Precision Spectroscopy, East China Normal University, Shanghai 200062, China

(Received 4 December 2023; accepted manuscript online 22 December 2023)

By numerically solving the two-dimensional semiconductor Bloch equation, we study the high-order harmonic emission of a monolayer ZnO under the driving of co-rotating two-color circularly polarized laser pulses. By changing the relative phase between the fundamental frequency field and the second one, it is found that the harmonic intensity in the platform region can be significantly modulated. In the higher order, the harmonic intensity can be increased by about one order of magnitude. Through time-frequency analysis, it is demonstrated that the emission trajectory of monolayer ZnO can be controlled by the relative phase, and the harmonic enhancement is caused by the second quantum trajectory with the higher emission probability. In addition, near-circularly polarized harmonics can be generated in the co-rotating two-color circularly polarized fields. With the change of the relative phase, the harmonics in the platform region can be altered from left-handed near-circularly polarization to right-handed one. Our results can obtain high-intensity harmonic radiation with an adjustable ellipticity, which provides an opportunity for syntheses of circularly polarized attosecond pulses.

DOI: 10.1088/0256-307X/41/1/014205

Interactions of intense laser pulses with gas, solid, and liquid can produce a series of nonlinear phenomena,^[1–3] including high-order harmonic generation (HHG).^[4–14] The harmonic spectrum of solids contains the information of interaction between light and matter. At present, it has been successfully applied to reconstruction of crystal band structures^[15–17] and transition dipole moments^[18–21] in reciprocal space, measurement of atomic position in real space,^[22] and imaging of Berry curvature.^[23] In addition to being a more easily integrated and compact extreme ultraviolet light source, the solid-state high-order harmonic generation is also an important method for synthesizing attosecond pulses.^[24–29] The ultra-short pulse can be used to study motion of electrons with high resolution on the attosecond time scale, which is an important and effective means to realize ultra-fast measurement. Moreover, by controlling polarization of harmonic emission, elliptical or circularly polarized HHG and attosecond pulses can be generated, which have important applications in x-ray magnetic circular dichroism, ultrafast spin dynamics, chiral recognition, and so on.^[30–32]

In 2011, Ghimire *et al.* first obtained non-perturbative solid-state HHG by using bulk ZnO crystals as target materials,^[33] which triggered a research boom of solid-state HHG. In the past decade, a large number of theoret-

ical and experimental studies related to HHG have been carried out for series of solid materials with different band gaps and properties.^[34–48] Among them, two-dimensional crystal materials have become popular target for solid high-order harmonics due to their unique electronic structure, excellent optical properties, strong electron-electron interaction, and negligible propagation effects.^[49,50] In addition, polarization characteristics of high-order harmonics of two-dimensional materials have a strong tunability, and it is possible to utilize two-dimensional materials to generate circularly polarized high-order harmonics.

Driving laser field pulse plays an important role in the generation process of high-order harmonics. By changing the parameters of the laser field, the efficiency and ellipticity of the solid harmonic can be controlled. With the change of the ellipticity of the laser field, the harmonic efficiency of the solid can appear atomic-like ellipticity and anomalous ellipticity dependence.^[51–54] Using multi-color linearly polarized combined pulses, Song *et al.* improved the harmonics in the plateau region of ZnO crystals by 2–3 orders of magnitude.^[55] Via varying the relative phase of orthogonally polarized two-color fields, Tang *et al.* increased the harmonic efficiency of ZnO crystals.^[56] Under monochromatic circularly polarized pulses, Chen *et al.* and Saito *et al.* obtained circularly polarized har-

*Corresponding authors. Email: kiddchen@126.com; scjiang@lps.ecnu.edu.cn; yangyj@jlu.edu.cn
© 2024 Chinese Physical Society and IOP Publishing Ltd

monics in graphene^[57] and crystalline solids,^[58] respectively. Through elliptically polarized pulses, Klemke *et al.* produced circularly polarized harmonics different from the polarization of the driving laser.^[59] He *et al.* studied the harmonic radiation process of MoS₂ with valley-selective circular dichroism, and they observed circularly polarized harmonics under counter-rotating two-color circularly polarized pulses.^[60]

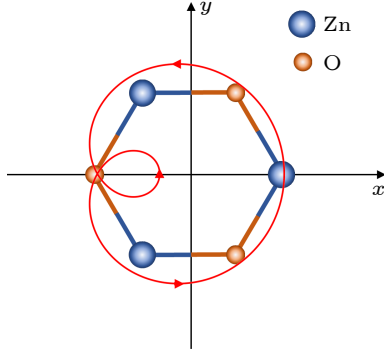


Fig. 1. Schematic diagram of the monolayer ZnO and co-rotating two-color field in real space. The counterclockwise rotation direction of the laser field is marked with red arrows.

Compared with the case of the counter-rotating two-color circularly polarized field,^[60,61] there are few studies on the co-rotating two-color circularly polarized laser in solids. However, according to the study of the interac-

tion between the co-rotational two-color field and the hydrogen molecular ion,^[62] it can be noticed that the near-circularly polarized harmonics of odd and even orders can be generated under the co-rotational two-color field, and the intensity is comparable to that of the counter-rotating circular polarized laser pulse. Therefore, the co-rotating two-color field is an effective tool to obtain high-intensity near-circularly polarized harmonics.

Based on this, we apply the co-rotating two-color circularly polarized field to the solid in our work, and systematically study the high-order harmonic radiation process of the monolayer ZnO crystal under the action of the co-rotating two-color field of 4000–2000 nm. Monolayer ZnO is a graphene-like two-dimensional honeycomb lattice.^[63] Figure 1 shows the relationship of the monolayer ZnO with the co-rotating two-color field in real space. The x and y components of the field are given (atomic units are always used in this study unless stated otherwise) as follows:

$$\begin{aligned} E_x(t) &= E_0 f(t) [\cos(\omega t) + \cos(2\omega t + \varphi)], \\ E_y(t) &= E_0 f(t) [\sin(\omega t) + \sin(2\omega t + \varphi)]. \end{aligned} \quad (1)$$

Here, $f(t)$ is the Gaussian envelope of the laser pulse with a full width at half maximum of 93.5 fs, corresponding to 7 optical periods (o.c.) of 4000 nm. $E_0 = 0.0105$ is the peak amplitude of the laser electric field, and $\omega = 0.01139$ is the angular frequency of the fundamental laser field (corresponding to the wavelength of 4000 nm), and φ represents the relative phase between the fundamental frequency field and the second one.

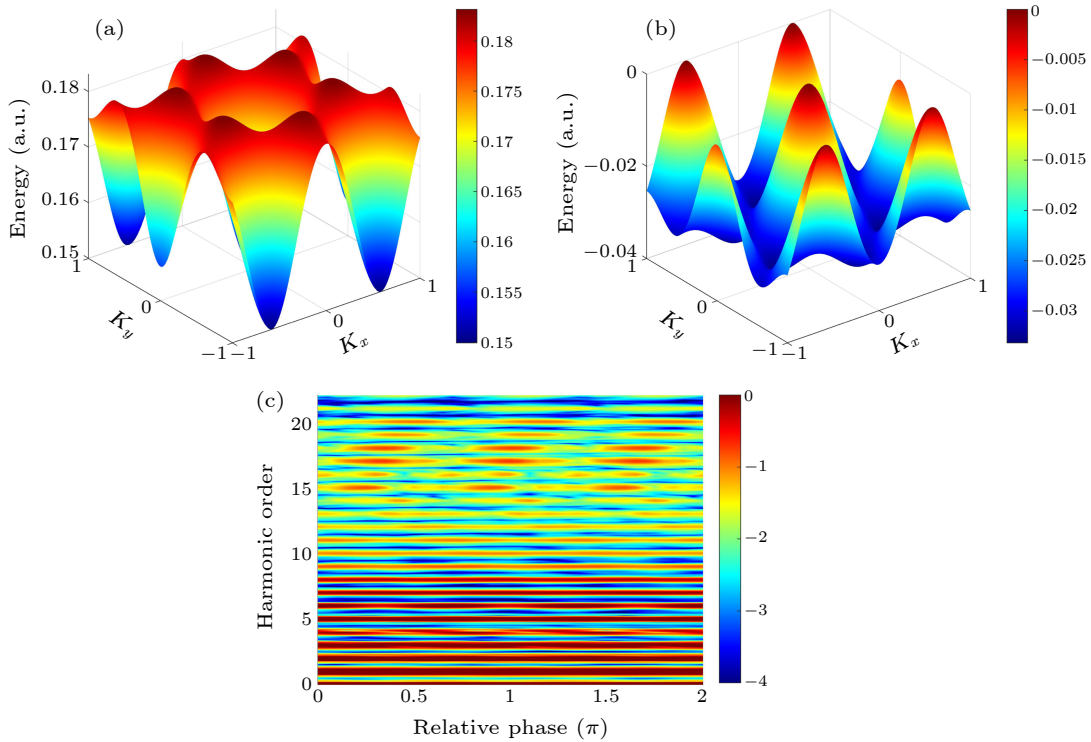


Fig. 2. The energy band structure of the monolayer ZnO: (a) conduction band, (b) valence band. (c) The variation of harmonic spectra of the monolayer ZnO with relative phase φ .

The monolayer ZnO can be modeled by the tight-binding model including the s orbital of Zn atom and p_x , p_y orbitals of the O atom. Figures 2(a) and 2(b) show the conduction band and valence band structures of the monolayer ZnO, respectively. The detailed parameters of constructing Hamiltonian can be found in the work of Hu *et al.*^[63] By numerically solving the two-dimensional semiconductor Bloch equation,^[64] we calculate the intensity of the total harmonic spectra of the monolayer ZnO as a function of relative phase φ , as shown in Fig. 2(c). In our simulation, the dephasing time is set to about a quarter cycle of the incident fundamental laser pulse. The x -axis

is the relative phase between the fundamental frequency field and the frequency doubling field, the y -axis is the harmonic order, and the color represents the harmonic intensity in the log scale. We can see that under the action of co-rotating field, both odd and even harmonics exist because the laser-crystal system does not have an order-2 dynamic symmetry.^[65,66] With the change of relative phase, the intensity of harmonics in the platform area is greatly modulated. Compared with the result of $\varphi = 0$, the yield of higher-order harmonics is significantly enhanced in the case of $\varphi = \pi$.

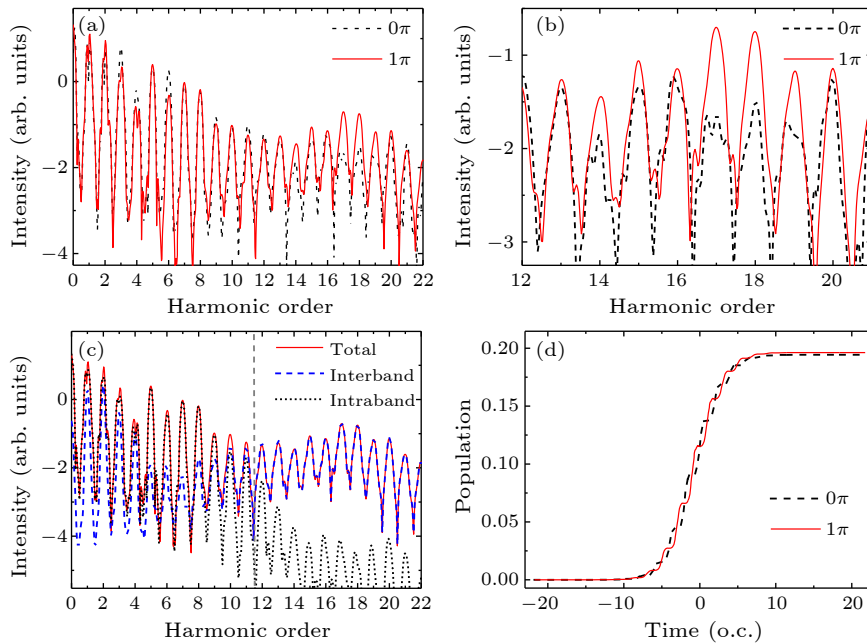


Fig. 3. (a) Comparison of harmonic spectra from $\varphi = 0$ (black dashed line) and $\varphi = \pi$ (red solid line). (b) The enlarged graph of (a). (c) The total harmonic spectrum (red solid line), the harmonic spectra generated by the interband (blue dashed line) and the intraband currents (black dotted line) when $\varphi = \pi$. (d) The electron population in the conduction band when $\varphi = 0$ (black dashed line) and $\varphi = \pi$ (red solid line).

In order to observe the difference of harmonic intensity under different relative phases more clearly, we compare the total harmonic spectra when $\varphi = 0$ (black dashed line) and $\varphi = \pi$ (red solid line) in Fig. 3(a). It can be seen that in the high-order region, the harmonic intensity of $\varphi = \pi$ can be increased by about one order of magnitude. Figure 3(c) shows the total harmonic (red solid line), interband harmonic (blue dashed line), and intraband harmonic (black dotted line) when $\varphi = \pi$, where the gray dotted line marks the harmonic order corresponding to the minimum band gap between the valence band and conduction one of the monolayer ZnO. It can be observed that the harmonics with energy lower than the minimum band gap are mainly dominated by intraband harmonics, the harmonics with energy higher than the minimum band gap are apparently originated from the interband polarization. Therefore, one can deduce that the harmonic enhancement in Fig. 3(a) may come from the modulation of the interband HHG by changing the relative phase. Since the harmonic

generation is closely related to the electron population, we analyze the evolution of the electron population of the system in the conduction band with time under different relative phases, as shown in Fig. 3(d). It can be seen that the conduction band electron population changes slightly when $\varphi = 0$ (black dashed line) and $\varphi = \pi$ (red solid line). Based on the above results, one can know that the enhancement of higher-order harmonics occurs under the condition that the ionization is almost unchanged. Therefore, we guess that this enhancement may be due to the modulation of the relative phase between the fundamental frequency field and the frequency doubling field on the electron and hole recollision trajectories.

In order to verify our view, we analyze the physical mechanism of harmonic generation from time-domain and frequency-domain information by using wavelet transform.^[67] The time-frequency analyses of harmonic emission for $\varphi = 0$ and $\varphi = \pi$ are given in Figs. 4(a) and 4(b), respectively. It can be seen that the time-

frequency distributions show different characteristics in the two cases. When $\varphi = 0$, there is a strong harmonic emission trajectory in each frequency doubling optical cycle. When $\varphi = \pi$, there are two strong emission trajectories in a frequency doubling optical cycle, and the harmonic frequency ranges of the two trajectories are significantly different. The harmonic frequency range of the first trajectory with earlier emission time is similar to that of $\varphi = 0$, while the energy of the second trajectory with later emission time is mainly concentrated in the high-order region. The intensity of the second trajectory is stronger than that of the first trajectory. Therefore, when $\varphi = \pi$, the enhancement of higher-order harmonic emission in the platform region of harmonic spectrum mainly comes from the second emission trajectory. The above results show that the relative phase of the co-rotating two-color circularly polarized laser field can control the emission trajectory and enhance the recollision probability.

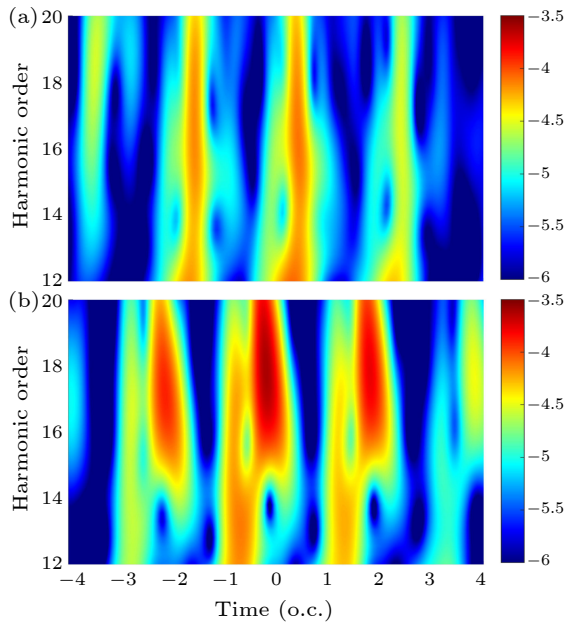


Fig. 4. Time-frequency analyses of HHG spectra for (a) $\varphi = 0$ and (b) $\varphi = \pi$.

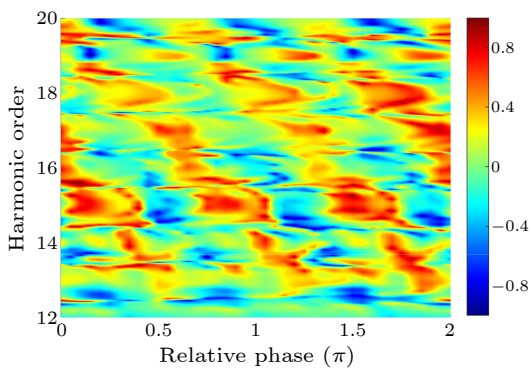


Fig. 5. Harmonic ellipticity in the plateau as a function of the relative phase φ .

In addition, we find that the relative phase φ of the

co-rotating two-color circularly polarized laser field can not only improve the harmonic intensity, but also regulate the harmonic ellipticity. Figure 5 shows the harmonic ellipticity of the plateau region at different relative phases. The ellipticity is represented by color. The right circular polarization is $+1$, which is indicated with red. The left circular polarization is -1 , expressed in blue. The harmonic ellipticity can be calculated by $e = (|j_+| - |j_-|) / (|j_+| + |j_-|)$,^[62,68,69] where $j_{\pm} = \frac{1}{\sqrt{2}}(j_x \pm ij_y)$, j_x and j_y are the x and y components of the laser-induced current inside the crystal in the frequency domain, respectively. It can be observed from the figure that the harmonic ellipticity is significantly affected by the relative phase. With the change of relative phase φ , the harmonics in the platform region are converted between left-handed circular polarization, linear polarization and right-handed circular polarization. Combined with the harmonic intensity at different relative phases given in Fig. 2(c), higher intensity near-circularly polarized harmonics can be obtained. For example, when $\varphi = 1.8\pi$, the 18th-order harmonic with a strong intensity close to the right-handed circular polarization can be produced; when $\varphi = 1.7\pi$, the 20th-order harmonic with a high intensity close to the left-handed circular polarization can be generated.

In summary, by numerically simulating the interaction between monolayer ZnO crystals and co-rotating two-color polarized laser pulses, we find that the relative phase between the fundamental frequency field and the second one has a significant modulation on the harmonic spectrum. Under some relative phase conditions, the higher-order harmonic intensity of the monolayer ZnO crystals can be significantly enhanced. Through analyses of electron time-dependent population under different relative phase conditions, it is proved that this enhancement cannot be attributed to the change of electron population. Further through time-frequency analysis, it is found that the higher-order harmonic enhancement at $\varphi = \pi$ is due to the additional emission trajectory contribution. In addition, the ellipticity of harmonics can also be modulated by the relative phase of the co-rotating two-color laser pulse. Under certain conditions, near-circularly polarized harmonics with high intensity can be obtained. Our results improve the direction for the generation of the polarization-controlled coherent high-frequency light source with high intensity in the experiment.

Acknowledgements. This work was supported by the Zhejiang Provincial Natural Science Foundation of China (Grant Nos. Y23A040001 and LY21F050001), the National Key Research and Development Program of China (Grant No. 2019YFA0307700), the National Natural Science Foundation of China (Grant Nos. 12074145, 11774219, 11975012, 12374029, 12304378, and 12204214), the Jilin Provincial Research Foundation for Basic Research, China (Grant No. 20220101003JC), the Foundation of Education Department of Liaoning Province, China (Grant No. LJKMZ20221435), and the National College Students Innovation and Entrepreneurship Training Program (Grant No. 202310350062). Yue Qiao acknowledges

the High Performance Computing Center of Jilin University for supercomputer time and the high performance computing cluster Tiger@IAMP.

References

- [1] Yuan H Y, Yang Y J, Guo F M, Wang J, Chen J G, Feng W, and Cui Z W 2023 *Opt. Express* **31** 24213
- [2] Yuan H Y, Yang Y J, Guo F M, Wang J, and Cui Z W 2022 *Opt. Express* **30** 19745
- [3] Li X F, Qiao Y, Wu D, Yu R X, Chen J G, Wang J, Guo F M, and Yang Y J 2024 *Chin. Phys. B* **33** 013302
- [4] Lewenstein M, Balcou P, Ivanov M Y, L'Huillier A, and Corkum P B 1994 *Phys. Rev. A* **49** 2117
- [5] Ndabashimiye G, Ghimire S, Wu M, Browne D A, Schafer K J, Gaarde M B, and Reis D A 2016 *Nature* **534** 520
- [6] Zeng A W and Bian X B 2020 *Phys. Rev. Lett.* **124** 203901
- [7] Yuan G L, Lu R F, Jiang S C, and Dorfman K 2023 *Ultrafast Sci.* **3** 0040
- [8] Jiang S C and Dorfman K 2020 *Proc. Natl. Acad. Sci. USA* **117** 9776
- [9] Yue L and Gaarde M B 2022 *J. Opt. Soc. Am. B* **39** 535
- [10] Fu T T, Zhou S S, Chen J G, Wang J, Guo F M, and Yang Y J 2023 *Opt. Express* **31** 30171
- [11] Fu T T, Qiao Y, Wang J, Guo F M, and Yang Y 2023 *Phys. Rev. A* **108** 033115
- [12] Qiao Y, Wang X, Li X, Wu L, Yu R, Guo F, Wang J, Chen J, and Yang Y 2023 *Opt. Express* **31** 36327
- [13] Jia G R, Zhao D X, Zhang S S, Yue Z W, Qin C C, Jiao Z Y, and Bian X B 2023 *Chin. Phys. Lett.* **40** 103202
- [14] Guo X L, Jin C, He Z Q, Zhao S F, Zhou X X, and Cheng Y 2021 *Chin. Phys. Lett.* **38** 123301
- [15] Lanin A A, Stepanov E A, Fedotov A B, and Zheltikov A M 2017 *Optica* **4** 516
- [16] Li L, Lan P, He L, Cao W, Zhang Q, and Lu P 2020 *Phys. Rev. Lett.* **124** 157403
- [17] Vampa G, Hammond T J, Thiré N, Schmidt B E, Légaré F, McDonald C R, Brabec T, Klug D D, and Corkum P B 2015 *Phys. Rev. Lett.* **115** 193603
- [18] Qiao Y, Huo Y, Liang H, Chen J, Liu W, Yang Y, and Jiang S 2023 *Phys. Rev. B* **107** 075201
- [19] Wu D, Li L, Zhan Y, Huang T, Cui H, Li J, Lan P, and Lu P 2022 *Phys. Rev. A* **105** 063101
- [20] Qiao Y, Huo Y Q, Jiang S C, Yang Y J, and Chen J G 2022 *Opt. Express* **30** 9971
- [21] Zhao Y T, Ma S Y, Jiang S C, Yang Y J, Zhao X, and Chen J G 2019 *Opt. Express* **27** 34392
- [22] Lakhota H, Kim H, Zhan M, Hu S, Meng S, and Goulielmakis E 2020 *Nature* **583** 55
- [23] Luu T T and Worner H J 2018 *Nat. Commun.* **9** 916
- [24] Antoine P, L'Huillier A, and Lewenstein M 1996 *Phys. Rev. Lett.* **77** 1234
- [25] Nourbakhsh Z, Tancogne-Dejean N, Merdji H, and Rubio A 2021 *Phys. Rev. Appl.* **15** 014013
- [26] Hu S Q and Meng S 2023 *Chin. Phys. Lett.* **40** 117801
- [27] Zhao X, Wang S J, Yu W W, Wei H, Wei C, Wang B, Chen J, and Lin C D 2020 *Phys. Rev. Appl.* **13** 034043
- [28] Zhou S S, Yang Y J, Yang Y, Suo M Y, Li D Y, Qiao Y, Yuan H Y, Lan W D, and Hu M H 2023 *Chin. Phys. B* **32** 013201
- [29] Tao W, Wang L, Song P, Xiao F, Wang J, Zheng Z, Zhao J, Wang X, and Zhao Z 2023 *Chin. Phys. Lett.* **40** 063201
- [30] Zhou X B, Lock R, Wagner N, Li W, Kapteyn H C, and Murnane M M 2009 *Phys. Rev. Lett.* **102** 073902
- [31] Cireasa R, Boguslavskiy A, Pons B *et al.* 2015 *Nat. Phys.* **11** 654
- [32] Graves C, Reid A, Wang T *et al.* 2013 *Nat. Mater.* **12** 293
- [33] Ghimire S, DiChiara A D, Sistrunk E, Agostini P, DiMauro L F, and Reis D A 2011 *Nat. Phys.* **7** 138
- [34] Lang Y, Peng Z, Liu J, Zhao Z, and Ghimire S 2022 *Phys. Rev. Lett.* **129** 167402
- [35] Jiang S C, Chen J G, Wei H, Yu C, Lu R, and Lin C D 2018 *Phys. Rev. Lett.* **120** 253201
- [36] Lv Y Y, Xu J, Han S, Zhang C, Han Y, Zhou J, Yao S H, Liu X P, Lu M H, Weng H *et al.* 2021 *Nat. Commun.* **12** 6437
- [37] Peng Z Y, Lang Y, Zhu Y L, Zhao J, Zhang D W, Zhao Z X, and Yuan J M 2023 *Chin. Phys. Lett.* **40** 054203
- [38] Lang Y, Peng Z Y, and Zhao Z X 2022 *Chin. Phys. Lett.* **39** 114201
- [39] Jia L, Zhang Z, Yang D Z, Liu Y, Si M S, Zhang G P, and Liu Y S 2020 *Phys. Rev. B* **101** 144304
- [40] Qiao Y, Chen J, Huo Y, Liang H, Yu R, Chen J, Liu W, Jiang S, and Yang Y 2023 *Phys. Rev. A* **107** 023523
- [41] Yu C, Zhang X, Jiang S, Cao X, Yuan G, Wu T, Bai L, and Lu R 2016 *Phys. Rev. A* **94** 013846
- [42] Jiang S C, Yu C, Chen J G, Huang Y W, Lu R F, and Lin C D 2020 *Phys. Rev. B* **102** 155201
- [43] Zhao J, Liu J, Wang X, Yuan J, and Zhao Z 2022 *Chin. Phys. Lett.* **39** 123201
- [44] Peng Q F, Peng Z Y, Lang Y, Zhu Y L, Zhang D W, Lü Z, and Zhao Z 2022 *Chin. Phys. Lett.* **39** 053301
- [45] Wang S, Guo J, He X, Liang Y, Xie B, Zhong S, Teng H, and Wei Z 2023 *Chin. Phys. B* **32** 063301
- [46] Shao J, Zhang C P, Jia J C, Ma J L, and Miao X Y 2019 *Chin. Phys. Lett.* **36** 054203
- [47] Zhao Y T, Xu X Q, Jiang S C, Zhao X, Chen J G, and Yang Y J 2020 *Phys. Rev. A* **101** 033413
- [48] Zhao Y T, Jiang S C, Zhao X, Chen J G, and Yang Y J 2020 *Opt. Lett.* **45** 2874
- [49] Liu H, Li Y, You Y S, Ghimire S, Heinz T F, and Reis D A 2017 *Nat. Phys.* **13** 262
- [50] Yoshikawa N, Tamaya T, and Tanaka K 2017 *Science* **356** 736
- [51] You Y S, Reis D A, and Ghimire S 2017 *Nat. Phys.* **13** 345
- [52] Tancogne-Dejean N, Mücke O, Kartner F, and Rubio A 2017 *Nat. Commun.* **8** 745
- [53] Zhang X, Li J, Zhou Z, Yue S, Du H, Fu L, and Luo H G 2019 *Phys. Rev. B* **99** 014304
- [54] Feng Y K, Shi S X, Li J B, Ren Y J, Zhang X, Chen J H, and Du H C 2021 *Phys. Rev. A* **104** 043525
- [55] Song X H, Yang S D, Zuo R X, Meier T, and Yang W F 2020 *Phys. Rev. A* **101** 033410
- [56] Tang D and Bian X B 2021 *Phys. Rev. B* **104** 104302
- [57] Chen Z Y and Qin R 2019 *Opt. Express* **27** 3761
- [58] Saito N, Xia P, Lu F, Kanai T, Itatani J, and Ishii N 2017 *Optica* **4** 1333
- [59] Klemke N, Mücke O D, Rubio A, Kärtner A F X, and Tancogne-Dejean N 2020 *Phys. Rev. B* **102** 104308
- [60] He Y L, Guo J, Gao F Y, and Liu X S 2022 *Phys. Rev. B* **105** 024305
- [61] Heinrich T, Taucer M, Kfir O, Corkum P, Staudte A, Ropers C, and Sivilis M 2021 *Nat. Commun.* **12** 3723
- [62] Qiao Y, Wu D, Chen J G, Wang J, Guo F M, and Yang Y J 2019 *Phys. Rev. A* **100** 063428
- [63] Hu Z J, Xie X C, Yang Z H, Wang Y H, and Jiang S C 2023 *Symmetry* **15** 1427
- [64] Qian C, Yu C, Jiang S, Zhang T, Gao J, Shi S, Pi H, Weng H, and Lu R 2022 *Phys. Rev. X* **12** 021030
- [65] Neufeld O, Podolsky D, and Cohen O 2019 *Nat. Commun.* **10** 405
- [66] Qian C, Jiang S, Wu T, Weng H, Yu C, and Lu R 2023 arXiv:2304.10109 [physics.optics]
- [67] Yu R X, Qiao Y, Li P, Wang J, Chen J G, Feng W, Guo F M, and Yang Y J 2023 *Chin. Phys. B* **32** 063302
- [68] Odzak S and Milošević D B 2015 *Phys. Rev. A* **92** 053416
- [69] Zhang X, Zhu X, Liu X, Wang D, Zhang Q, Lan P, and Lu P 2017 *Opt. Lett.* **42** 1027